Physics Letters B 747 (2015) 36–42

Contents lists available at ScienceDirect

Physics Letters B

www.elsevier.com/locate/physletb

# Equation of state and viscosities from a gravity dual of the gluon plasma

R. Yaresko [a,b,*], B. Kämpfer [a,b]

[a] Helmholtz-Zentrum Dresden-Rossendorf, POB 51 01 19, 01314 Dresden, Germany
[b] TU Dresden, Institut für Theoretische Physik, 01062 Dresden, Germany

ARTICLE INFO

*Article history:*
Received 4 June 2013
Received in revised form 30 April 2015
Accepted 16 May 2015
Available online 19 May 2015
Editor: J.-P. Blaizot

*Keywords:*
Gravity dual
Holography
Gluon plasma

ABSTRACT

Employing new precision data of the equation of state of the SU(3) Yang–Mills theory (gluon plasma) the dilaton potential of a gravity-dual model is adjusted in the temperature range (1–10)$T_c$ within a bottom-up approach. The ratio of bulk viscosity to shear viscosity follows then as $\zeta/\eta \approx \pi \Delta v_s^2$ for $\Delta v_s^2 < 0.2$ and achieves a maximum value of 0.94 at $\Delta v_s^2 \approx 0.3$, where $\Delta v_s^2 \equiv 1/3 - v_s^2$ is the non-conformality measure and $v_s^2$ is the velocity of sound squared, while the ratio of shear viscosity to entropy density is known as $(4\pi)^{-1}$ for the considered set-up with Hilbert action on the gravity side.



## 1. Introduction

With the advent of new precision data [1], which extend previous lattice QCD gauge theory evaluations [2,3] for the pure gluon plasma to a larger temperature range, a tempting task is to seek for an appropriate gravity dual model. While such an approach does not necessarily provide new insights in the pure SU(3) Yang–Mills equation of state above the deconfinement temperature $T_c$, it however allows to calculate, without additional ingredients, further observables, e.g. transport coefficients. (This is in contrast to quasiparticle approaches which require additional input to access transport coefficients [4].) In considering an ansatz of gravity + scalar as framework of effective dual models to pure non-abelian gauge thermo-field theories within a bottom-up approach one has to adjust either the potential of the dilaton field, or a metric function, or the dilaton profile.

The improved holographic QCD (IHQCD) model, developed in [5–8] (for a review cf. [9]) is a particularly successful realization of such a setting. The potential of IHQCD [8] was constructed to match the t'Hooft limit Yang–Mills $\beta$ function to two-loop order (which determines the functional form and two parameters) in the near-conformal (small t'Hooft coupling) region, while the zero-temperature (large t'Hooft coupling) behavior is fixed by demanding confinement and a linear glueball spectrum. A potential smoothly interpolating between the two asymptotic regions was shown in [8] to well reproduce the $N_c = 3$ Yang–Mills plasma equation of state [2], where remaining free parameters were fixed by comparing to the latent heat and scaled pressure from the lattice. Within IHQCD, zero-temperature confining geometries exhibit a first-order thermodynamic phase transition [7].

A different type of dilaton potentials was considered in [10], where near the boundary the potential accounts for a massive scalar field and the spacetime asymptotes to pure $AdS_5$. The potential parameters were matched to the velocity of sound as suggested by the hadron resonance gas model and the dimension of $\mathrm{Tr}\, F^2$ at a finite scale [11] and reproduce the velocity of sound of $2+1$ flavor QCD, whereas in [12] the matching to the SU(3) Yang–Mills equation of state [2] has been accomplished. In IHQCD, the marginal operator dual to $\phi$ is $\mathrm{Tr}\, F^2$ [5], while in [10,11] and here the dual operator $\mathcal{O}$ is interpreted as a relevant deformation of the boundary theory Lagrangian. In [13], instead of the dilaton potential, an ansatz for a metric function of the five-dimensional gravity action is selected and consequences for the boundary theory are explored (Such an approach suffers however from the conceptual shortcoming that the dilaton potential and thus the action depend on the temperature, while, according to the gauge/gravity duality, the bulk action should be independent of the boundary theory state).

The previous benchmark lattice data [2] (up to $4.5T_c$) and further SU($N_c$) data for $N_c \leq 8$ [14] (up to $3.5T_c$) and $N_c \leq 6$ [15] (up to $4T_c$) are for $N_c = 3$ now supplemented and extended up to $1000T_c$ [1]. Here we are going to adjust precisely the dilaton potential to the new lattice data [1] in the temperature range up

* Corresponding author.
*E-mail address:* r.yaresko@hzdr.de (R. Yaresko).

http://dx.doi.org/10.1016/j.physletb.2015.05.034

to $10T_c$, thus catching the strong-coupling regime, as envisaged as relevant also in [16]. We discard completely a recourse to the $\beta$ function. Such an approach can be considered as a convenient parameterization of the equation of state. Once the potential is adjusted, it qualifies for further studies, e.g. of transport coefficients. Our goal is accordingly the quantification of the bulk viscosity in the LHC relevant region, in particular near to $T_c^+$, and a comparison with results of the quasiparticle model [4].

According to holography, $SU(N_c)$ Yang–Mills theory at finite $N_c$ must be described by quantum string theory, which has not yet been completely established. Since in the large-$N_c$ and large t'Hooft coupling limits quantum string theory reduces to classical gravity, one presently resorts to a gravitation theory in a five-dimensional space, constructed in such a manner to accommodate certain selected features of the holographically emerging boundary field theory. As in the models [9,10], one often considers the AdS/QCD correspondence as deformation of the original AdS/CFT correspondence [17] by additional (relevant or marginal) operators which allow a qualitative study of QCD or Yang–Mills properties in the strong-coupling regime. Conclusions for the latter theories should be drawn with caution: For instance, in the perturbative regime of the (large-$N_c$) boundary theory, the gravity theory is expected to become strongly coupled and, consequently, finite string scale corrections may arise; if one also leaves the t'Hooft limit, stringy loop corrections may matter. (It is known that equilibrium thermodynamics of $SU(N_c)$ Yang–Mills depend only weakly on $N_c$, see [14] and references therein.) Having these disclaimers in mind, we nevertheless study quantitatively the bulk viscosity in a bottom-up setting matched solely to $N_c = 3$ Yang–Mills thermodynamics within $(1-10)T_c$.

The potential asymptotics of Gubser–Nellore [10,11] and IHQCD [9] models are different both in the near-boundary region, i.e. at high temperatures and also deep in the bulk, i.e. at low temperatures. When adjusting the potential in an intermediate region suitable for (1–10)$T_c$ one would like to know whether it is important to incorporate a certain kind of asymptotics, or whether they have little influence. Put another way, to what extent does a fit to lattice data on (1–10)$T_c$ determine the potential? Here, we do not attempt to solve the general problem of computing the potential from a given equation of state, but instead show that various potentials which contain a certain unique relevant section lead to nearly identical equations of state in the corresponding temperature region.

Transport properties of the matter produced in relativistic heavy-ion collisions at RHIC and LHC are important to characterize precisely such novel states of a strongly interacting medium besides the equation of state. The impact of the bulk viscosity on the particle spectra and differential elliptic flows has been recently discussed in [18] and found to be sizeable in [19], in particular for higher-order collective flow harmonics. The bulk viscosity enters also a new soft-photon emission mechanism [20] via the conformal anomaly, thus offering a solution to the photon-$v_2$ puzzle (cf. [20] for details and references). Compilations of presently available lattice QCD results of viscosities can be found in [4].

## 2. The set-up

The action $S = \frac{1}{16\pi G_5}\int d^5x\sqrt{-g}\left\{R - \frac{1}{2}(\partial\phi)^2 - V(\phi)\right\}$ (the Hawking–Gibbons term is omitted) leads, with the ansatz for the infinitesimal line element squared in Riemann space $ds^2 = \exp\{2A\}(d\vec{x}^2 - hdt^2) + \exp\{2B\}h^{-1}L^2d\phi^2$, to the field equations quoted in [10] under (25a–25c); the equation of motion (25d) follows from the derivative of (25c) with insertion of (25a–25c). Here, the coordinate transformation $dz = L\exp\{B-A\}d\phi$ has been employed to go from the Fefferman–Graham coordinate $z$ in the infinitesimal line element squared $ds^2 = \exp\{2A\}(-h\,dt^2 + d\vec{x}^2 + h^{-1}\,dz^2)$ to a gauged radial coordinate expressed by the dilaton field $\phi$ which requires the introduction of a length scale $L$. The metric functions are thus to be understood as $A(\phi;\phi_H)$, $B(\phi;\phi_H)$ and $h(\phi;\phi_H)$, and a prime means in the following the derivative with respect to $\phi$. These equations can be rearranged by defining $Y_1 = A - A_H$, $Y_2 = A' + U$, $Y_3 = A'' + \frac{1}{2}U'$, $Y_4 = B - B_H$, $Y_5 = \exp(4A_H - B_H)\int_{\phi_H}^{\phi} d\tilde{\phi}\exp(-4A + B)$, where the subscript $H$ denotes the value of a function at the horizon and $U \equiv V/(3V')$, to change the mixed boundary value problem into an initial value problem, given by

$$Y_1' = Y_2 - U, \tag{1}$$

$$Y_2' = Y_3 + \frac{1}{2}U', \tag{2}$$

$$Y_3' = \frac{1}{2}U'' + \frac{Y_3 - \frac{1}{2}U'}{(Y_2-U)Y_2}\left((Y_3 - \frac{1}{2}U')(3Y_2 - 2U) + (4Y_2 - \frac{U'}{U})(Y_2-U)^2 + \frac{Y_2}{6U}(2Y_2 - U)\right), \tag{3}$$

$$Y_4' = \frac{6(Y_3 - \frac{1}{2}U') + 1}{6(Y_2 - U)}, \tag{4}$$

$$Y_5' = \exp\{-4Y_1 + Y_4\} \tag{5}$$

which is integrated from the horizon $\phi_H - \epsilon$, to the boundary $\epsilon$ with the initial values $Y_i = 0$ at $\phi_H - \epsilon$. The limit $\epsilon \to 0^+$ has to be taken to obtain the entropy density $s$ and the temperature $T$

$$G_5 s = \frac{1}{4}\exp(3A_H), \tag{6}$$

$$LT = -\frac{1}{4\pi}\frac{\exp(A_H - B_H)}{Y_5(\epsilon)}, \tag{7}$$

where $A_H = \frac{\log\epsilon}{\Delta-4} - Y_1(\epsilon)$ and $B_H = -\log(-\epsilon[\Delta-4]) - Y_4(\epsilon)$. This set[1] ensures the boundary conditions $h(\phi=0) = 1$ and $h(\phi_H) = 0$ as well as the AdS asymptotic limits $A(\phi) = \frac{\log\phi}{\Delta-4}$ (we set $L\Lambda = 1$ [10]) and $B(\phi) = -\log(-\phi[\Delta-4])$ at $\phi \to 0^+$. The boundary asymptotics of $A$ and $B$ assume $L^2V(\phi) \approx -12 + (\Delta[\Delta-4]/2)\phi^2$ for small $\phi$, where $\Delta$ is the scaling dimension of the conformality-breaking operator of the boundary theory. We consider $2 < \Delta < 4$, selecting the upper branch of the mass dimension relation $L^2M^2 = \Delta(\Delta-4)$ and restricting to relevant operators. Hence, the Breitenlohner–Freedman bound $L^2M^2 \geq -4$ [21] is respected and renormalizability on the gauge theory side is ensured. The quantities $Y_i(\epsilon)$ depend on the horizon position $\phi_H$, implying in particular $s(\phi_H)$ and $T(\phi_H)$, thus providing the equation of state $s(T)$ in parametric form.

## 3. Equation of state

To compare with the lattice results [1] of the relevant thermodynamical quantities (i) sound velocity squared $v_s^2 = \frac{d\log T}{d\log s}$, (ii) scaled entropy density $s/T^3$, (iii) scaled pressure $p/T^4$, and

[1] The system (1)–(5) enjoys some redundancy. It can be reduced by introducing $X \equiv 1/4A' = 1/(4[Y_2-U])$, $Y \equiv h'/(4hA') = Y_5'/(4Y_5[Y_2-U])$ which leads to two coupled first-order ODEs for the scalar invariants $X(\phi;\phi_H)$ and $Y(\phi;\phi_H)$ according to [7]. Eliminating $Y$ in this system leads to a second-order ODE for $X$, equivalent to the "master equation" in [10]. Two additional quadratures are then needed to obtain the thermodynamics via $LT = \frac{V(\phi_H)}{\pi V(\phi_0)}\exp(A(\phi_0) + \int_{\phi_0}^{\phi_H} d\phi[\frac{1}{4X} + \frac{2}{3}X])$ and $G_5 s = \frac{1}{4}\exp(3A(\phi_0) + \frac{3}{4}\int_{\phi_0}^{\phi_H} d\phi\frac{1}{X})$. The set (1)–(5) does not need such additional quadratures.

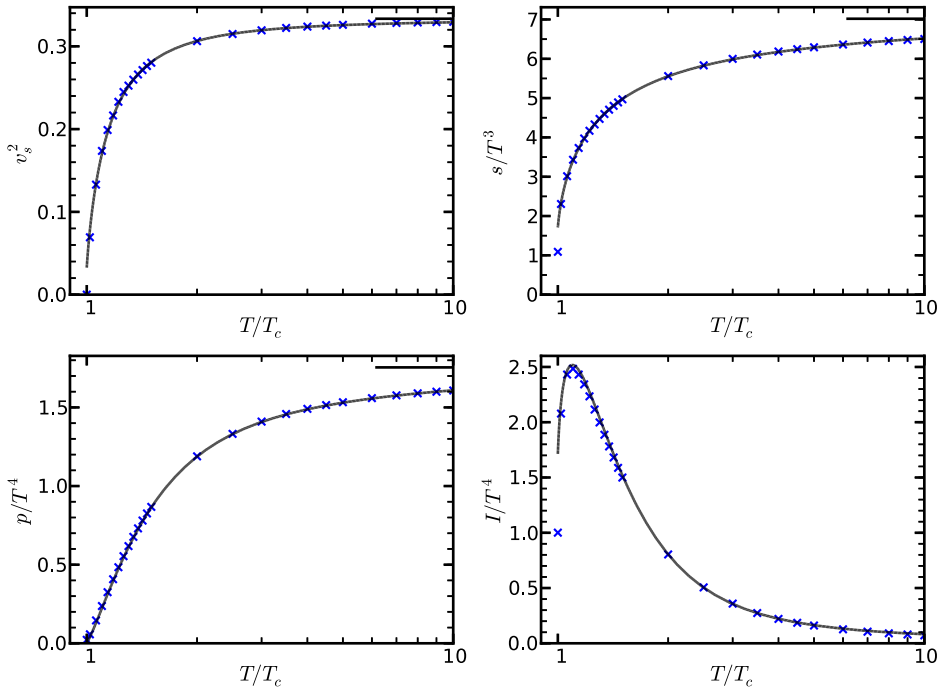


**Fig. 1.** The sound velocity squared $v_s^2$ (left top panel), scaled entropy density $s/T^3$ (right top panel), scaled pressure $p/T^4$ (left bottom panel), and scaled interaction measure $I/T^4$ (right bottom panel) as functions of $T/T_c$ for the potential $v_1$ (8) with optimized parameters (10). The lattice data (symbols) are from [1]. The horizontal lines in the upper right corners depict the respective Stefan–Boltzmann limits.

(iv) scaled interaction measure $I/T^4 = s/T^3 - 4p/T^4$ (all as functions of $T/T_c$) one must adjust the scale $T_c$ and the 5D Newton's constant $G_5$ (actually, the dimensionless combinations $LT_c$ and $G_5/L^3$ are needed). In the present bottom-up approach, we employ a new potential designed to reproduce the data [1] in the temperature region $(1\text{–}10)T_c$,

$$v_1(\phi) = \frac{V'(\phi)}{V(\phi)} = \begin{cases} \frac{-L^2M^2}{12}\phi + i_1\phi^3 & \text{for } \phi \le \phi_m, \\ \gamma + s_1[\mathrm{erf}(s_2(\phi - s_3)) - 1] & \text{for } \phi \ge \phi_m, \end{cases} \quad (8)$$

as an ansatz and optimize the parameters $\phi_m$, $s_{1,2,3}$ and $\gamma$. Since we are not interested in the high-temperature regime $T > 10T_c$, we choose a simple interpolation from $\phi = 0$ to $\phi = \phi_m$. The latter value is taken as a fit parameter and fixes $L^2M^2$ and $i_1$ by the requirement that $v_D$ should be differentiable at $\phi_m$. The critical temperature $LT_c$ is determined by $T_c = T(\phi_H^c)$ with $\phi_H^c$ from the pressure

$$p(\phi_H) = \int_{\infty}^{\phi_H} d\tilde{\phi}_H s(\tilde{\phi}_H) \frac{dT}{d\tilde{\phi}_H}, \quad (9)$$

via $p(\phi_H^c) = 0$. This is the prescription discussed in detail in [7] for the first-order phase transition to a thermal gas configuration at $T < T_c$. According to [6,7] the boundary theory at $T < T_c$ is confining and gapped if $\gamma > \sqrt{2/3}$ and, equivalently, $LT(\phi_H)$ is U shaped, with a global minimum at $\phi_H^{min}$, implying $T(\phi_H^c) > T(\phi_H^{min})$, see Fig. A.3. The construction ensures a minimum free energy for $T < T_c$ (thermal gas with $p = 0$) and $T > T_c$ (large black hole branch which continues in the UV region). In (9), $p(\infty) = 0$ for a "good" IR singularity requires $\gamma < 2\sqrt{2/3}$.

Our results are exhibited in Fig. 1 for the optimized parameter set

| $v$ | $\phi_m$ | $s_1$ | $s_2$ | $s_3$ | $\gamma$ | $G_5/L^3$ |
|---|---|---|---|---|---|---|
| $v_1$ | 1.3444 | 0.3954 | 0.6723 | 2.7358 | 0.8222 | 1.1100 |

(10)

The velocity of sound is independent of $G_5$ which steers the number of degrees of freedom, thus being important for entropy density, energy density $e$, pressure and interaction measure. In asymptotically free theories, the $T^4$ term dominates $s$, $e$ and $p$ at large temperatures; it is subtracted in the interaction measure making it a sensible quantity. (Unlike the IHQCD model our ansatz does not catch pQCD features in the deep UV. That is the reason for our restriction to $T < 10T_c$.) The appearance of a maximum of $I/T^4$ at $T/T_c \approx 1.1$ is related to a turning point of $p/T^4$ as a function of $\log T$. Position and height of $I/T^4$ – the primary quantity in lattice calculations – are sensible characteristics of the equation of state. The dropping of $I/T^4$ at larger temperatures signals the approach towards conformality. (Since in conformal theories $v_s^2 = 1/3$, the quantity $\Delta v_s^2 = 1/3 - v_s^2$ is termed non-conformality measure; also here, the dominating $T^4$ terms at large temperatures drop out.) Inspection of Fig. 1 unravels the nearly perfect description of the lattice data [1]. Note that, by construction, $p/T^4$ always slightly underestimates the lattice data for $T \to T_c^+$, since $p(\phi_H^c) = 0$, while $p(T_c)/T_c^4|_{lattice} = 0.0222$ [1]. We find $\Delta s(T_c)/T_c^3 \approx 1.7$ for the scaled latent heat.

## 4. Viscosities

Irrespectively of the dilaton potential $V(\phi)$, the present set-up with Hilbert action $R$ for the gravity part delivers $\eta/s = (4\pi)^{-1}$ [23,24] for the shear viscosity $\eta$, often denoted as KSS value [25]. (See [26] for the original calculation. Inclusion of higher-order curvature corrections can decrease the KSS value [27].) In contrast, the bulk viscosity to entropy density ratio $\zeta/s$ has a pronounced temperature dependence. Following [23] we calculate $\zeta$ from the relation

$$\frac{\zeta}{\eta}\Big|_{\phi_H} = \frac{1}{9U(\phi_H)^2} \frac{1}{|p_{11}(\epsilon)|^2}, \quad (11)$$

where the asymptotic value $p_{11}(\epsilon)$ of the perturbation $p_{11}$ of the 11-metric coefficient is obtained by integrating

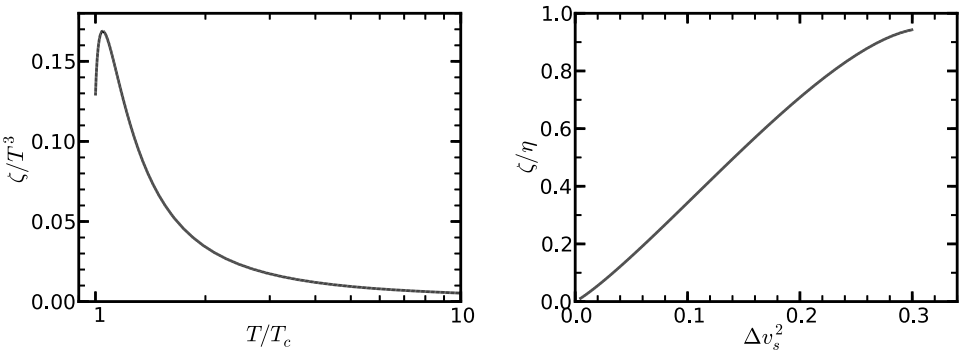


**Fig. 2.** The scaled bulk viscosity $\zeta/T^3$ as a function of the temperature (left panel) and the ratio $\zeta/\eta$ as a function of the non-conformality measure (right panel).

$$p_{11}'' + \left(\frac{1}{3(Y_2-U)} + 4(Y_2-U) - 3Y_4' + \frac{Y_5'}{Y_5}\right) p_{11}' + \frac{Y_5'}{Y_5}\frac{Y_3 - \frac{1}{2}U'}{Y_2-U} p_{11} = 0 \tag{12}$$

from the horizon $\phi_H - \epsilon$ to the boundary $\epsilon$ with initial conditions $p_{11}(\phi_H - \epsilon) = 1$ and $p_{11}'(\phi_H - \epsilon) = 0$ and $\epsilon \to 0^+$. Equivalently [28], the bulk viscosity can be obtained from the Eling–Oz formula [24]

$$\frac{\zeta}{\eta}\Big|_{\phi_H} = \left(\frac{d\log s}{d\phi_H}\right)^{-2} = \left(\frac{1}{v_s^2}\frac{d\log T}{d\phi_H}\right)^{-2}. \tag{13}$$

Our results are exhibited in Fig. 2. The scaled bulk viscosity $\zeta/T^3$ has a maximum at $1.05T_c$ (which is slightly below the maximum of $I/T^4$) and drops rapidly for increasing temperatures, see left panel of Fig. 2. Remarkable is the almost linear section of $\zeta/\eta$ as a function of the non-conformality measure $\Delta v_s^2$ (see right panel), as already suggested in [29] and observed, in particular at high temperatures, in numerous holographic models [30,31]; for further reasoning on such a linear behavior within holography approaches cf. [32]. A non-linear behavior occurs in a small temperature interval $1 \le T/T_c < 1.05$, i.e. for $\Delta v_s^2 > 0.22$, see right panel of Fig. 2. The maximum value of $\zeta/\eta \approx 0.94$ at $\Delta v_s^2 \approx 0.3$ depends fairly sensitively on the details of the equation of state for $T \to T_c^+$.

Interesting is the relation $\zeta/\eta \propto 1.2\pi\Delta v_s^2$ for $0.025 < \Delta v_s^2 < 0.2$ which follows numerically and is specific for the selected potential parameters. This corresponds to the temperature interval $1.05 < T/T_c < 2$; extending the fit to $1.05 < T/T_c < 10$ we find $\zeta/\eta \approx \pi\Delta v_s^2$. The IHQCD model [33] yields also $\zeta/\eta \propto 1.2\pi\Delta v_s^2$, i.e. it is on top of the curve in the right panel Fig. 2, but stops at $\Delta v_s^2(T_c) \approx 0.22$.

The viscosity ratio accommodates the Buchel bound $\zeta/\eta \ge 2\Delta v_s^2$ [30] and agrees surprisingly well on a qualitative level with the result of [4] in the interval $1.05 < T/T_c < 2$. There, a quasi-particle approach has been employed which needs, beyond the equation-of-state adjustment, further input: In [4] it is the dependence of the relaxation time on the temperature which causes a change from the linear relation $\zeta/\eta \propto \Delta v_s^2$ near $T_c^+$, i.e. for large values of $\Delta v_s^2$, to a quadratic dependence in the weak-coupling regime [34] at large temperatures corresponding to small values of $\Delta v_s^2$. Note also the shift of the linear section of $\zeta/\eta$ in [4] by a somewhat larger off-set which can cause a descent violation of the Buchel bound, which is not unexpected with respect to [35].

## 5. Robustness of the bulk viscosity

### 5.1. Definition of the transition temperature

If one is interested in the thermodynamics of the deconfined phase a theoretically sound determination of $T_c$ can be related to the Hawking–Page transition and to the construction of [7], as strictly applied in section 3. Fitting the data [1], we observe [36] $\tilde{T}_c = (1+\varepsilon)T_{min}$ with positive $\varepsilon < 10^{-2}$ and $\tilde{T}_c$ from the pressure loop (see Fig. A.1, inset in left bottom panel). One could be tempted, therefore, to ignore the numerically tiny difference of the proper thermodynamic first-order transition temperature $\tilde{T}_c$ and $T_{min}$ and to use $T_{min}$ instead. In fact, then one can easily reproduce the lattice data [1], as shown in [36], e.g. by a potential similar to [11], distorted by polynomial terms,

$$L^2 V_{IV}(\phi) = -12\cosh(\gamma\phi) + (6\gamma^2 + \frac{1}{2}\Delta[\Delta-4])\phi^2 + \sum_{i=2}^{5}\frac{c_{2i}}{(2i)!}\phi^{2i}, \tag{14}$$

whereby the original Gubser–Nellore potential [10], referred to as $V_I$, follows for $c_{2i} = 0$.

### 5.2. Generating nearly equivalent potentials

The scheme of employing the holographic principle here consists of mapping $V(\phi \in [\phi_0, \phi_H]) \Rightarrow T(\phi_H), s(\phi_H) \Rightarrow s(T)$,[2], i.e. the complete non-local potential properties enter the local thermodynamics. Since we are interested in $s/T^3$ as a function of $T/T_c$ in the restricted interval $T = (1\ldots10)T_c$, one can ask whether near-boundary properties of $V(\phi)$ are irrelevant. We provide evidence that this is indeed the case, at least for $\varepsilon \ll 1$, where one can tentatively neglect the difference of $T_{min}$ and $\tilde{T}_c$, and ignoring the IR behavior. To substantiate this claim, let us consider a special one-parameter potential $V_s(\phi;\phi_s)$ which contains as relevant part the section $V_I(\phi \gtrsim \phi_m)$ where $\phi_m = 0.55$ means a value of $\phi_H$ corresponding to $10\tilde{T}_c$ determined by the potential $V_I$. The relevant section of $V_I$ is now up or down shifted by a parameter $\phi_s$, and $L^2 V_{int}(\phi;\phi_s) = -12 + \frac{1}{2}L^2 m_{int}^2(\phi_s)\phi^2 + b(\phi_s)\phi^4$ is an interpolating section from the boundary $\phi_0$ to the matching point $\phi_m + \phi_s$. The conditions $V_I(\phi_m) = V_{int}(\phi_m + \phi_s;\phi_s)$, $V_I'(\phi_m) = V_{int}'(\phi_m + \phi_s;\phi_s)$ fix $L^2 m_{int}^2$ and $b$. The Breitenlohner–Freedman bound $-4 \le L^2 m_{int}^2 \le 0$ restricts the possible values of $\phi_s$ for given $V_{int}$ and $\phi_m$; in our example, $-0.165 \le \phi_s \le 0.4$. To quote a few numbers, the left-most shift $\phi_s = -0.165$ yields $L^2 m_{int}^2 = -3.927$, $\Delta = 2.271$, $LT_{min} = 1.81 \times 10^{-2}$, while the right-most shift $\phi_s = 0.4$ yields $L^2 m_{int}^2 = -0.098$, $\Delta = 3.975$, $LT_{min} =$

[2] Here, the boundary position is denoted by $\phi_0$, being at $\phi = 0$ for the potential (14), while in the IHQCD model [5–8] it is at $\phi = -\infty$. Because of this, the approximate symmetry of the equation of state under constant shifts $\phi \to \phi + \phi_s$, discussed here, is *exact* in IHQCD [9].

$3.46 \times 10^{19}$.[3] Despite of a huge variation of $LT_{min}$, dimensionless thermodynamic quantities $T/T_{min}$ and $s/T^3$ as functions of $\phi_H - \phi_s$ are within very narrow corridors with relative variations (depending on $\phi_H - \phi_s$ and parametrically on $\phi_s$) of less than $4 \times 10^{-2}$ for $T/T_{min}$ and $5 \times 10^{-4}$ for $s/T^3$. From the Eling–Oz formula (13), one infers an analogous behavior of $\zeta/\eta$ as a function of $\phi_H - \phi_s$, meaning that the potentials $V_s$ deliver a nearly unique equation of state and viscosity ratio in the considered temperature interval. We therefore argue that all precise fits of $V(\phi)$ to lattice data deliver, up to a linear shift, nearly equivalent potentials in the selected temperature region and, in particular, nearly the same $\zeta/\eta$ vs. $\Delta v_s^2$.

At the end of this degression on the role of $T_c$ and the conjectured robustness of the bulk viscosity we mention that we are not able to fit precisely (8) with parameters (10) by $V'/V$ emerging from the potential (14) with $\gamma > \sqrt{2/3}$. Apparently, (14) and the proper $T_c$ definition along [7] with well defined IR behavior seem to fail a precise match to the data [1]. In the Appendix we present a potential which accommodates also lattice data below $\tilde{T}_c$.

## 6. Discussion and summary

Inspired by the AdS/CFT correspondence we employ an AdS/QCD hypothesis and adjust, in a bottom-up approach, the dilaton potential parameters at lattice gauge theory thermodynamics data for the pure SU(3) gauge field sector. We describe several variants to accurately reproduce the data of [1] in the LHC relevant temperature region from $T_c$ up to $10T_c$. Conceptually, the match to the thermal gas solution at $T < T_c$ is most satisfactory and can be accomplished by a properly designed dilaton potential, which precisely catches the lattice data above $T_c$. Giving up the criteria of [6,7] for a zero-temperature confining boundary theory with a gapped excitation spectrum in the deep IR, one can construct a thermodynamic first-order phase transition with a perfect match of lattice data within $(0.7 - 10)T_c$. When focusing on $T > T_c$ the Gubser–Nellore potential form is comfortable for fitting the lattice data with an ad hoc choice of a scale identified with $T_c$. Clearly this latter variant ignores the physics of the boundary theory below and at $T_c$.

Despite of such ambiguities, we find the bulk viscosity at and above $T_c$ as fairly robust, with deviations of at most 6% for $T/T_c \leq 1.02$ and otherwise less than 2%, supposed $T_c$ is a proper first-order transition temperature (if not, the bulk viscosity can significantly vary, depending upon the choice of the scale, see also [22]).

Within the non-conformal region $1 \leq T/T_c \leq 10$, where the non-conformality measure is $0.2 > \Delta v_s^2 > 0.004$ and the interaction measure is $2.48 > I/T^4 > 0.07$, an almost linear dependence $\zeta/\eta \approx \pi \Delta v_s^2$ on the non-conformality measure $\Delta v_s^2$ is observed, as already argued in [29] and found within holographic approaches [30,31] and in [4] within a quasi-particle approach to the pure gauge sector of QCD.

We mention further that one can identify a relevant section of the potential which determines the equation of state in a selected temperature interval. Shifting, within certain limits that relevant section, the equation of state and the bulk viscosity are marginally modified.

Extensions towards including quark degrees of freedom and subsequently non-zero baryon density, i.e. to address full QCD, have been outlined and explored in [37]. The Veneziano limit of QCD is investigated in a more string theory inspired setting in [38]. Incorporating additional degrees of freedom (which are aimed at mimicking an equal number of quarks and anti-quarks) within the present set-up, one essentially has to lower $G_5/L^3$ in adjusting the extensive and intensive densities. Since the viscosities scale with $L^3/G_5$ [23] (as the entropy density does, too) the corresponding ratios $\zeta/s$ and $\zeta/\eta$ would stay unchanged, if the same potential would apply and the same behavior of the sound velocity would be used as input. However, as stressed above, $\zeta/\eta$ depends rather sensitively on the actual potential $V(\phi)$ and its parameters. Since QCD does not display a first-order phase transition at zero baryon density, dedicated separate investigations are required to adjust the dilaton potential to current lattice data. (The results in [23] yield $\zeta/\eta \approx 0.98\pi\Delta v_s^2$ for $\Delta v_s^2 < 0.28$ with a maximum of $\zeta/\eta \approx 0.75$ at $\Delta v_s^2 \approx 0.26$, i.e. values comparable to the pure glue case.)

On the gravity side, inclusion of terms beyond the Hilbert action would cause a temperature dependence of the ratio $\eta/s$ [39] which is needed to furnish the transition into the weak-coupling regime [40] at large temperatures. It is an open question whether such higher-order curvature corrections also lead to a quadratic dependence of the viscosity ratio on the non-conformality measure [34].

In summary, we adjust the dilaton potential exclusively at new lattice data for SU(3) gauge theory thermodynamics and calculate holographically the bulk viscosity. The ratio of the bulk to shear viscosity obeys, in the strong-coupling regime, a linear dependence on the non-conformality measure for temperatures above $1.05T_c$, while at $T_c$ it has a maximum of 0.94. Our result, which is based on some fine tuning of the dilaton potential to precision lattice data, agrees well with previous holographic approaches based on former lattice data, such as the IHQCD model, or studies with the Gubser–Nellore potential types which envisaged qualitatively capturing QCD features.

It would be interesting to employ the numerical findings of our holographically motivated guess, even if they are related to the pure gauge theory (with the disclaimers mentioned in the introduction), e.g. in the modelings [18–20] of heavy-ion collisions to elucidate their impact on observables. Our potential(s) may also serve as a suitable background, e.g. for various holographic mesons.

## Acknowledgements

Inspiring discussions with M. Bluhm, M. Huang, E. Kiritsis, K. Redlich, C. Sasaki, U.A. Wiedemann, P.M. Heller and L.G. Yaffe are gratefully acknowledged. The work is supported by BMBF grant 05P12CRGH1 and European Network HP3-PR1-TURHIC (grant number 283286).

## Appendix A. Including confined-phase lattice data

The potential $v_1$ in (8) can be modified to reproduce also the presently available lattice data in the confined phase:

$$v_2 = \begin{cases} \frac{-L^2M^2}{12}\phi + i_1\phi^3 & \text{for } \phi \leq \phi_m, \\ \gamma + s_1[\tanh(s_1(\phi - s_2)) - 1] & \\ \quad + p_1 e^{p_2(\phi - p_3)^2} & \text{for } \phi \geq \phi_m. \end{cases} \tag{A.1}$$

This parametrization is inspired by the desired behavior of $v_s^2$ as function of $\phi_H$.[4] Performing a fit to lattice data for $0.7 \leq T/T_c \leq 10$

[3] There is a subtlety here: due to the small, but finite, influence of the UV region $T^s_{min} \neq T^s(\phi^{min}_{H,V_l} + \phi_s)$, however $|T^s_{min} - T^s(\phi^{min}_{H,V_l} + \phi_s)|/T^s_{min} < 1.3 \times 10^{-3}$. For the procedure described in the text, $s/T^3(T_{min})$ varies between 1.11 and 1.32. For $T > T_{min}$, (and also if one uses $T^s_{min} = T^s(\phi^{min}_{H,V_l} + \phi_s)$) $T/T_{min}$ and $s/T^3$ stay within the corridors mentioned in the text.

[4] The parametrization (A.1) is superior to the one given in the appendix of [36], since a better description of $v_s^2$ for $T < T_c$ is accomplished.

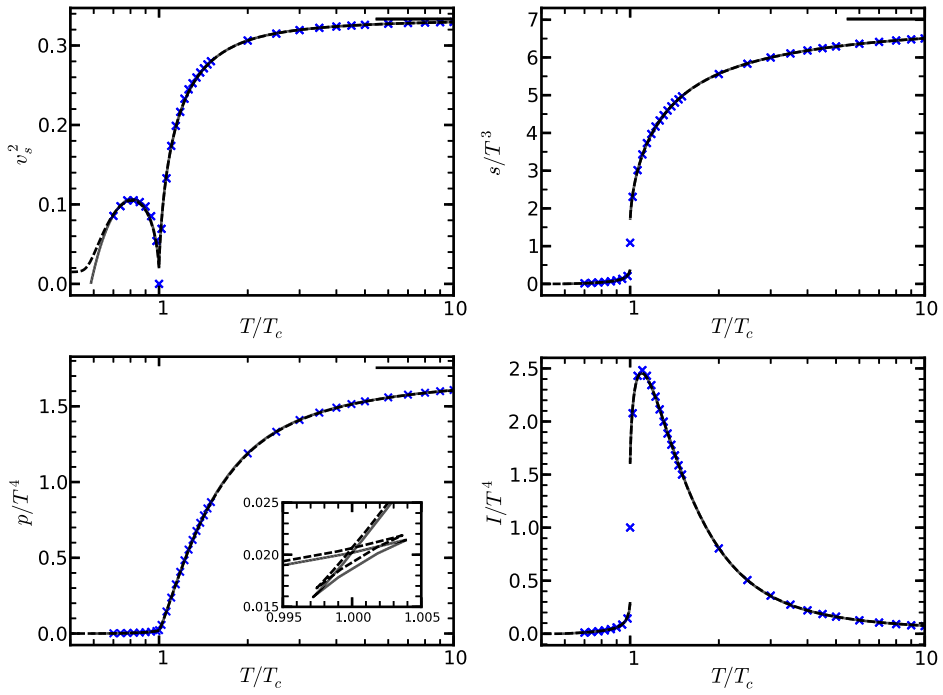


**Fig. A.1.** The same as Fig. 1 but extending the lattice data points and model calculation into the confined phase for the potential $v_2$ (A.1) with parameters (A.2). Solid curves: $v_{2a}$, dashed curves: $v_{2b}$. The unstable/metastable branches are not plotted, unless in the inset of the pressure panel, where the standard loop structure is displayed for $p/T^4$ with $p$ calculated from (9).

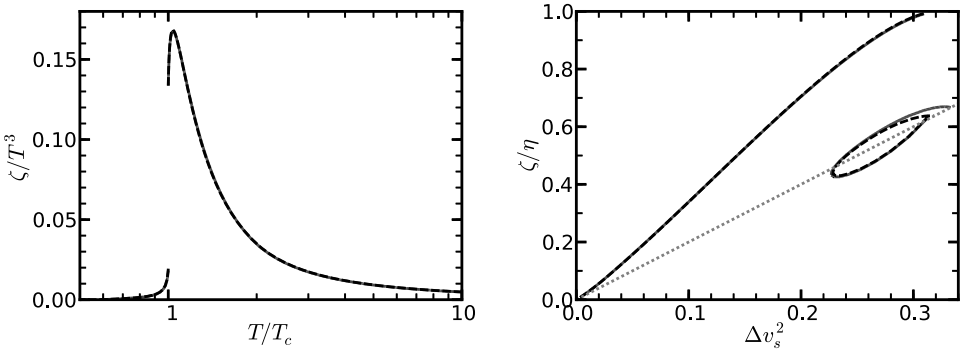


**Fig. A.2.** The scaled bulk viscosity $\zeta/T^3$ as a function of the temperature (left panel) and the ratio $\zeta/\eta$ as a function of the non-conformality measure (right panel). Line codes are the same as in Fig. A.1. The grey dotted line in the right panel depicts the Buchel bound.

and identifying $T_c$ with $\tilde{T}_c$, which is determined by the intersection of the high-temperature and low-temperature branches of the pressure (9) combined with $T(\phi_H)$, we find the parameters

| $v$ | $\phi_m$ | $s_1$ | $s_2$ | $\gamma$ | $p_1$ | $p_2$ | $p_3$ | $G_5/L^3$ |
|---|---|---|---|---|---|---|---|---|
| $v_{2a}$ | 2.3523 | 0.4452 | 6.9382 | $\sqrt{2/3}$ | 0.7526 | 0.1707 | 4.6707 | 1.1125 |
| $v_{2b}$ | 2.3171 | 0.4259 | 6.5929 | 0.7979 | 0.6982 | 0.1864 | 4.6011 | 1.1116 |

(A.2)

The resulting equation of state is exhibited in Fig. A.1. In the direct vicinity of $T_c$ the model calculation deviates from the lattice data on a 5% level in the high- and low-temperature phases; otherwise the fit is near-perfect. Unlike the potential $v_1$ (8) which facilitates a monotonous increase of $LT(\phi_H)$ for $\phi_H > \phi_H^{min}$, $LT(\phi_H)$ from $v_{2a}$ (with fixed $\gamma = \sqrt{2/3}$) runs to a constant value, while for $v_{2b}$ it is dropping, see Fig. A.2. That is the potentials $v_{2a}$ and $v_{2b}$ leave the IR physics of the boundary theory unsettled, which however does not play any role for the description of the lattice data for $T > 0.7T_c$ as seen from Fig. A.1. The potential $v_{2a}$ can be regarded as the best compromise between two mutually exclusive options: $v_1$, a zero-temperature confining and gapped boundary theory and $v_{2b}$, a boundary theory with smooth and finite pressure for $0 < T < T_c$; in the classification of [7], the model $v_{2a}$ is zero-temperature confining and has a partially discrete spectrum. For both parameter sets (A.2) we find the scaled latent heat $\Delta s(T_c)/T_c^3 \approx 1.3$ which compares well with $\Delta s(T_c)/T_c^3 \approx 1.4$ found in lattice calculations (see [1] and references therein).

The bulk viscosity resulting from the ansatz (A.1) with the parameters (A.2) is exhibited in Fig. A.2. The maximum $\zeta/\eta \approx 1$ lies at $\Delta v_s^2 \approx 0.31$. We notice the jump at $T_c$ due to the first-order phase transition; $\zeta/T^3$ is rapidly dropping for smaller temperatures; $\zeta/\eta$ vs. $\Delta v_s^2$ displays a hook which we would not consider a reliable result since the setting at $T < T_c$ might not be trustworthy. Below $T_c$, in the interval $0.76 \lesssim T/T_c \lesssim 0.998$, the viscosity ratio $\zeta/\eta$ violates the Buchel bound (see right panel of Fig. A.2). A similar behavior was found in [23] for the potential $V_I$ adjusted to the equation of state of $2+1$ flavor QCD.

Fig. A.3 summarizes the dependence of the temperature as a function of $\phi_H$. The global minimum for $v_1$ (8) is quite shallow (the anticipated U shape becomes better evident when displaying

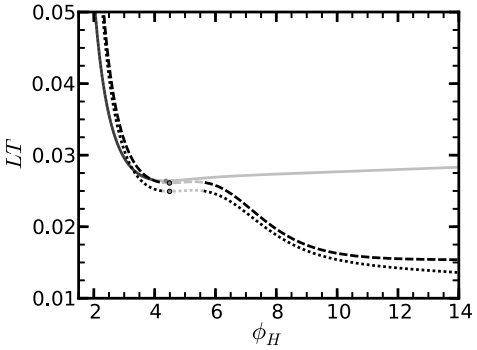


**Fig. A.3.** The temperature as a function of $\phi_H$ for the potentials $v_1$ (8) with parameters (10) (solid curve) as well as $v_{2a}$ (dashed curve) and $v_{2b}$ (dotted curve), see (A.1) and (A.2). Light grey portions of the curves denote the unstable/metastable regions of the equation of state, while dots mark the positions of $\phi_H^{min}$.

$LT$ as a function of $\log \phi_H/\phi_H^{min}$). The local minima for $v_{2a,b}$ (A.1) are also very shallow. Thus, $T_{min} \approx T_c$ or $\tilde{T}_c$ follows.

## References


[1] Sz. Borsanyi, G. Endrodi, Z. Fodor, S.D. Katz, K.K. Szabo, J. High Energy Phys. 1207 (2012) 056.
[2] G. Boyd, J. Engels, F. Karsch, E. Laermann, C. Legeland, M. Lutgemeier, B. Petersson, Nucl. Phys. B 469 (1996) 419.
[3] M. Okamoto, et al., CP-PACS Collaboration, Phys. Rev. D 60 (1999) 094510.
[4] M. Bluhm, B. Kämpfer, K. Redlich, Phys. Lett. B 709 (2012) 77;
M. Bluhm, B. Kämpfer, K. Redlich, Phys. Rev. C 84 (2011) 025201.
[5] U. Gursoy, E. Kiritsis, J. High Energy Phys. 0802 (2008) 032.
[6] U. Gursoy, E. Kiritsis, F. Nitti, J. High Energy Phys. 0802 (2008) 019.
[7] U. Gursoy, E. Kiritsis, L. Mazzanti, F. Nitti, J. High Energy Phys. 0905 (2009) 033.
[8] U. Gursoy, E. Kiritsis, L. Mazzanti, F. Nitti, Nucl. Phys. B 820 (2009) 148.
[9] U. Gursoy, E. Kiritsis, L. Mazzanti, G. Michalogiorgakis, F. Nitti, Lect. Notes Phys. 828 (2011) 79.
[10] S.S. Gubser, A. Nellore, Phys. Rev. D 78 (2008) 086007.
[11] S.S. Gubser, A. Nellore, S.S. Pufu, F.D. Rocha, Phys. Rev. Lett. 101 (2008) 131601.
[12] J. Noronha, Phys. Rev. D 81 (2010) 045011.
[13] D. Li, S. He, M. Huang, Q.S. Yan, J. High Energy Phys. 1109 (2011) 041.
[14] M. Panero, Phys. Rev. Lett. 103 (2009) 232001.
[15] S. Datta, S. Gupta, Phys. Rev. D 82 (2010) 114505.
[16] J. Alanen, K. Kajantie, V. Suur-Uski, Phys. Rev. D 80 (2009) 126008.
[17] J.M. Maldacena, Adv. Theor. Math. Phys. 2 (1998) 231;
S.S. Gubser, I.R. Klebanov, A.M. Polyakov, Phys. Lett. B 428 (1998) 105;
E. Witten, Adv. Theor. Math. Phys. 2 (1998) 253.
[18] K. Dusling, T. Schafer, Phys. Rev. C 85 (2012) 044909.
[19] J. Noronha-Hostler, G.S. Denicol, J. Noronha, R.P.G. Andrade, F. Grassi, Phys. Rev. C 88 (2013) 044916.
[20] G. Basar, D. Kharzeev, V. Skokov, Phys. Rev. Lett. 109 (2012) 202303.
[21] P. Breitenlohner, D.Z. Freedman, Phys. Lett. B 115 (1982) 197;
P. Breitenlohner, D.Z. Freedman, Ann. Phys. 144 (1982) 249.
[22] R. Yaresko, B. Kämpfer, Acta Phys. Pol. B, Proc. Suppl. 7 (2014) 137.
[23] S.S. Gubser, S.S. Pufu, F.D. Rocha, J. High Energy Phys. 0808 (2008) 085.
[24] C. Eling, Y. Oz, J. High Energy Phys. 1106 (2011) 007.
[25] P. Kovtun, D.T. Son, A.O. Starinets, Phys. Rev. Lett. 94 (2005) 111601.
[26] G. Policastro, D.T. Son, A.O. Starinets, Phys. Rev. Lett. 87 (2001) 081601.
[27] A. Buchel, R.C. Myers, A. Sinha, J. High Energy Phys. 0909 (2009) 084.
[28] A. Buchel, J. High Energy Phys. 1105 (2011) 065;
A. Buchel, U. Gursoy, E. Kiritsis, J. High Energy Phys. 1109 (2011) 095.
[29] A. Buchel, Phys. Rev. D 72 (2005) 106002.
[30] A. Buchel, Phys. Lett. B 663 (2008) 286.
[31] A. Cherman, A. Nellore, Phys. Rev. D 80 (2009) 066006;
A. Yarom, J. High Energy Phys. 1004 (2010) 024.
[32] I. Kanitscheider, K. Skenderis, J. High Energy Phys. 0904 (2009) 062.
[33] U. Gursoy, E. Kiritsis, G. Michalogiorgakis, F. Nitti, J. High Energy Phys. 0912 (2009) 056.
[34] P.B. Arnold, C. Dogan, G.D. Moore, Phys. Rev. D 74 (2006) 085021.
[35] A. Buchel, Phys. Rev. D 85 (2012) 066004.
[36] R. Yaresko, B. Kämpfer, arXiv:1306.0214v3.
[37] O. DeWolfe, S.S. Gubser, C. Rosen, Phys. Rev. D 83 (2011) 086005;
O. DeWolfe, S.S. Gubser, C. Rosen, Phys. Rev. D 84 (2011) 126014.
[38] M. Järvinen, E. Kiritsis, J. High Energy Phys. 1203 (2012) 002;
T. Alho, M. Järvinen, K. Kajantie, E. Kiritsis, K. Tuominen, J. High Energy Phys. 1301 (2013) 093;
D. Arean, I. Iatrakis, M. Järvinen, E. Kiritsis, Phys. Lett. B 720 (2013) 219;
T. Alho, M. Järvinen, K. Kajantie, E. Kiritsis, C. Rosen, K. Tuominen, J. High Energy Phys. 1404 (2014) 124.
[39] S. Cremonini, U. Gursoy, P. Szepietowski, J. High Energy Phys. 1208 (2012) 167.
[40] P.B. Arnold, G.D. Moore, L.G. Yaffe, J. High Energy Phys. 0011 (2000) 001;
P.B. Arnold, G.D. Moore, L.G. Yaffe, J. High Energy Phys. 0305 (2003) 051.